

# Optimising Deep Neural Networks for Tumour Diagnosis Algorithms Based on Improved MRFO Algorithm

Binbin Han<sup>1</sup>, Fuliang Zhang<sup>2,\*</sup>, Zhenyun Chang<sup>1</sup> and Fang Feng<sup>1</sup>

<sup>1</sup>Tianjin Tianshi College, Tianjin 301700, China

<sup>2</sup>Tianjin Nankai Hospital, Tianjin 300100, China

## Abstract

**INTRODUCTION:** Cancer has become one of the most prevalent diseases with the highest mortality rate in the world, and timely detection and early acceptance of medical therapeutic interventions are effective means of controlling the progression of cancer patients and improving their post-intervention outcomes.

**OBJECTIVES:** To make the defects of incomplete features, low accuracy and low real-time performance of current tumour diagnosis methods.

**METHODS:** This paper proposes a tumour diagnosis method based on the improved MRFO algorithm to improve the optimization process of DBN network parameters. Firstly, the diagnostic features are extracted by analysing the tumour diagnosis identification problem; then, the manta ray foraging optimization algorithm is improved by combining the good point set initialization strategy, the adaptive control parameter strategy and the distribution estimation strategy, and the tumour diagnostic model based on the improved manta ray foraging optimization algorithm to optimize the parameters of the depth confidence network is constructed; finally, the high accuracy and real-time performance of the proposed method are verified by the analysis of simulation experiments.

**RESULTS:** The results show that the proposed method improves the accuracy of the diagnostic model.

**CONCLUSION:** Addresses the problem of poor accuracy and real-time availability of tumour diagnostic methods.

**Keywords:** tumour diagnosis algorithms, adaptive control parameter strategy, distribution estimation strategy, manta ray foraging optimisation algorithm, deep confidence networks

Received on 20 February 2024, accepted on 26 March 2024, published on 08 April 2024

Copyright © 2024 B. Han *et al.*, licensed to EAI. This is an open access article distributed under the terms of the [CC BY-NC-SA 4.0](https://creativecommons.org/licenses/by-nc-sa/4.0/), which permits copying, redistributing, remixing, transformation, and building upon the material in any medium so long as the original work is properly cited.

doi: 10.4108/eetpht.10.5147

\*Corresponding author. Email: tjzfl123@163.com

## 1. Introduction

Oncology and cancer have become the major causes of death worldwide, and have become a major public health problem, seriously affecting the quality of life and health of human beings [1]. Although the global mortality rate of oncology cancer has shown a decreasing trend due to early screening and the continuous improvement of comprehensive treatment, the incidence of oncology cancer has been increasing year by year, and there is a trend of rejuvenation, and the epidemiological situation is not optimistic [2]. Oncology cancer has become one of the highest prevalence and mortality rates in the world, and timely detection and early acceptance of medical

therapeutic interventions are effective means of controlling the progression of oncology cancer patients and improving their post-intervention [3]. Therefore, exploring effective ways to improve oncology cancer census and exploring effective ways to improve early diagnosis rate are of great significance to improve the survival rate and mortality rate of oncology cancer patients [4]. At the same time, accurate diagnosis of tumour cancers is a particularly important advance in curing tumour cancers, and being able to accurately diagnose tumour cancers has an extremely important significance in prolonging the survival time of patients and improving their quality of life [5].

Tumour cancer diagnosis is essentially a classification and recognition problem [6], by taking X-ray photographs of the tumour cancer, acquiring ware medical images, then

extracting features from the region of interest, and finally using certain algorithms to classify the extracted features, so as to differentiate whether the tumour is benign or malignant, and thus determine whether it is suffering from tumour cancer [7]. Currently, tumour cancer diagnosis and recognition methods include region-based methods, contour evolution-based methods, machine learning-based methods, statistical-based methods, and methods based on multi-resolution analysis [8]. Machine learning based methods are mainly divided into generative model based methods and discriminative model based methods [9]. Generative model-based methods include Markov Random Fields, Gaussian Mixture Models [10]; discriminative model-based methods include Support Vector Machines, Random Forests, Deep Neural Networks [11]. Literature [12] used traditional statistical clustering methods to cluster patient case data to solve the problem of classification prediction of diseases; Literature [13] used correlation analysis to explore the relationship between disease recurrence and basic patient indicators; Literature [14] proposed an incremental decision tree algorithm based on the fast decision tree algorithm to deal with a large amount of routine medical data; Literature [15] used KNN, neural network, decision tree and Bayesian classification methods to explore the heart disease data and conducted a method comparison test; Literature [16] applied the association rules and neural network classification methods in data mining to the prediction problem of breast tumour, and the experimental analysis yielded a good prediction result; Literature [17] proposed a medical data clustering classification based on the combination of neural network, genetic algorithm and fuzzy classification algorithm, and analysed the characteristic data structure and features of medical data; Literature [18] used the LSSVM method to solve the classification problem of tumour diagnosis and identification in medical data; Literature [19] proposed a method combining SVM with autoregressive integrative sliding average model for predicting the patient's blood glucose value; Literature [20] applied the support vector machine algorithm, random forest algorithm, CatBoost algorithm to the breast tumour diagnosis and identification, through analysis and comparison of the results of different algorithms, CatBoost algorithm has the best performance.

In response to the above literature analysis, the existing oncology cancer diagnostic methods have the following shortcomings:

- 1) the traditional expert system diagnostic methods are subjective, and the diagnostic results are unscientific [21];
- 2) the existing oncology cancer diagnostic methods based on machine learning algorithms are unable to reflect the non-linear relationship between pathological features and whether or not one has breast cancer, and are unable to establish an accurate diagnostic model [22];
- 3) the existing diagnostic models have robustness is poor and lacks generalisation [23].

Deep Belief Networks (DBN)[23] DBN algorithm is a type of neural network for machine learning, which can be used for both unsupervised and supervised learning. DBN is

a probabilistic generative model as opposed to the traditional discriminative model of neural networks, where the generative model creates a joint distribution between observations and labels. By training the weights between its neurons, the whole neural network can be made to generate training data according to the maximum probability. The group intelligent optimization algorithm mainly simulates the group behaviours of insects, beasts, birds and fish, which search for food according to a certain cooperative way, and each member of the group constantly changes the direction of the search by learning from its own experience and the experience of the other members, which achieves the effect of obtaining the global optimal results [24]. The combination of deep confidence network and intelligent optimization algorithm makes the tumour cancer recognition effective, which makes the research of tumour cancer recognition model based on intelligent optimization algorithm optimization to improve the deep confidence network become the hotspot of experts' research.

Aiming at the problems existing in the current tumour cancer recognition method, this paper proposes a tumour cancer recognition method based on the intelligent optimization algorithm optimizing the improved deep confidence network. The main contributions of this paper are:

- 1) extracting the features of tumour cancer diagnosis and recognition by describing the problem of tumour cancer diagnosis and recognition, and constructing the feature system of tumour cancer diagnosis and recognition;
- 2) constructing the tumour cancer diagnosis and recognition model by combining the improved intelligent optimization algorithm and the deep confidence network;
- 3) verifying the method of this paper through simulation, which has a higher recognition accuracy and recognition real-time performance.

## 2. Analysis of the problem of diagnostic identification of tumours

### 2.1. Data sources

This paper carries out research on tumour diagnosis recognition methods for breast tumour diagnosis problems. Breast tumour diagnostic data comes from the UCI machine learning library, with a total of 569 samples, of which the benign breast tumour data samples are 357 cases and the malignant breast tumour data samples are 212 cases. Each diagnostic sample data contains 30 feature data and 1 diagnostic result of benign and malignant classification, which are associated with the benign and malignant classification of breast tumour tumours. The examination method applied for this diagnosis is cell sectioning of the lesion area of breast tumour patients in order to obtain microscopic images of the nuclei of multiple cells in the section of the lesion part [25].

## 2.2. Diagnostic Characterisation Data

In this paper, firstly, the nuclear microscopic images of multiple lines of eight sections of the same lesion site were processed separately to obtain the radius of the nucleus, texture of the nucleus, perimeter of the nucleus, area of the nucleus, smoothness of the nucleus, compactness of the nucleus, convexity of the nucleus, number of points of the nucleus, symmetry of the nucleus, and the degree of nuclear fracture of the nucleus in the nuclear microscopic image of each cell [26]. Then the nuclear micrographic image data of multiple cells belonging to the same lesion site section were averaged, standard deviation and worst value [27], i.e., the required 30 feature data. The 30 feature data include mean value of nucleus radius X1, mean value of nucleus texture X2, mean value of nucleus circumference X3, mean value of nucleus area X4, mean value of nucleus smoothness X5, mean value of nucleus compactness mean value X6, nucleus concavity mean value X7, nucleus depression point

mean value X8, nucleus symmetry mean value X9, nucleus fracture mean value X10, nucleus radius standard deviation X11, nucleus texture standard deviation X12, nucleus perimeter standard deviation X13, nucleus area standard deviation X14, nucleus smoothness standard deviation X15, nucleus compactness standard deviation X16, standard deviation of nucleus concavity X17, standard deviation of nucleus concavity point X18, standard deviation of nucleus symmetry X19, standard deviation of nucleus fracture X20, worst value of nucleus radius X21, worst value of nucleus texture X22, worst value of nucleus perimeter X23, worst value of nucleus area X24, worst value of nucleus smoothness X25, worst value of nucleus compactness X26, worst value of nucleus concavity X27, worst value of nucleus concavity point X28, worst value of nucleus symmetry X29, worst value of nucleus breakage X30. The principle of influencing factors selection is shown in Figure 1.

Var	Definition	Value range	Var	Definition	Value range
X1	Radius average	6.98~27.42	X16	Compactness SD	0.019~0.245
X2	Texture average	9.71~30.72	X17	Depression SD	0~0.396
X3	Circumference average	43.79~188.5	X18	Dent points SD	0~0.2
X4	Area average	143.5~2501	X19	Symmetry SD	0.106~0.528
X5	Smoothness average	0.053~0.16	X20	Crack SD	0.0078~0.0789
X6	Compactness average	0.019~0.245	X21	Worst radius	7.93~36.04
X7	Depression average	0~0.427	X22	Worst texture	12.02~49.54
X8	Dent points average	0~0.2	X23	Worst circumference	50.41~251.2
X9	Symmetry average	0.106~0.304	X24	Worst area	185.2~4254
X10	Crack average	0.05~0.097	X25	Worst smoothness	0.071~0.2226
X11	Radius SD	0.1115~2.873	X26	Worst compactness	0.027~1.058
X12	Texture SD	0.3602~4.885	X27	Worst depression	0~1.252
X13	Circumference SD	0.757~21.98	X28	Worst dent points	0~0.291
X14	Area SD	6.802~542.2	X29	Worst symmetry	0.156~0.6638
X15	Smoothness SD	0.0022~0.1354	X30	Worst crack	0.055~0.2075

Figure 1. Diagnostic features of breast cancer

## 3. Deep confidence network (D CN)

Deep Belief Networks (DBN) [28] consist of multiple Restricted Boltzmann Machines (RBM) layers, a typical type of neural network is shown in Figure These networks are restricted to a visible layer and a hidden layer with connections between the layers but not between the units within the layers. The hidden layer units are trained to capture the correlation of higher order data exhibited in the visible layer, the exact structure of which is shown in Figure 2. As can be seen from Figure 2, the input layer  $V$  and the hidden layer  $h^1$  constitute the first layer of the RBM, and the input data is mapped through the activation

function to the hidden layer  $h_1$ , which is input to the second layer of the RBM (the hidden layer  $h_1$  and the hidden layer  $h_2$ ), and the data is passed through the hidden layer sequentially to reach the output layer.

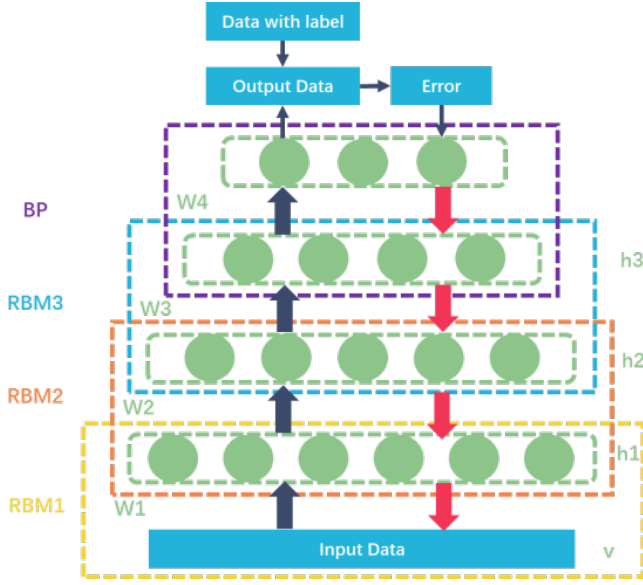


Figure 2. DBN structure

(1) Calculate the RBM energy function. Assuming that  $\theta = (\omega, a, b)$  is the DBN network parameter, the energy function of RBM is expressed as:

$$E(v, h|\theta) = -\sum_{i=1}^n a_i v_i - \sum_{j=1}^m b_j h_j - \sum_{i=1}^n \sum_{j=1}^m v_i \omega_{ij} h_j \quad (1)$$

Where,  $(v, h)$  is the state value of DBN,  $\omega$  is the connection weight of the visible and hidden layers,  $a$  and  $b$  are the bias of the visible and hidden layers respectively, and the hidden and visible layer states are binary states, i.e.  $v \in \{0, 1\}$  and  $h \in \{0, 1\}$ .

(2) The stochastic gradient method is used to solve the DBN network parameters  $\theta$ . The corresponding parameters  $\theta^*$  are obtained by solving the maximum of the log-likelihood function:

$$\theta^* = \arg_{\theta} \max L(\theta) = \arg_{\theta} \max \sum_{k=1}^K \ln p(v^k | \theta) \quad (2)$$

where  $K$  is the number of training samples.

(3) The joint probability distribution function can be determined from the energy function:

$$p(v, h|\theta) = \frac{e^{-E(v, h|\theta)}}{Z(\theta)} \quad (3)$$

$$Z(\theta) = \sum_v \sum_h e^{-E(v, h|\theta)} \quad (4)$$

(4) Determine the state of the visible layer. The activation probability of the  $j$ th network node of the hidden layer is

$$p(h_j = 1|v, \theta) = \text{sigmoid}\left(b_j + \sum_{i=1}^n v_i \omega_{ij}\right) \quad (5)$$

(5) Determine the hidden layer state. The activation probability of the  $i$ th network node of the visual layer is

$$p(v_i = 1|h, \theta) = \text{sigmoid}\left(a_i + \sum_{j=1}^n h_j \omega_{ij}\right) \quad (6)$$

(6) According to Gibbs sampling theorem, the RBM parameter  $\theta$  is updated with the following formula:

$$\Delta \omega_{ij} = \frac{\partial \log p(v)}{\partial \omega_{ij}} = \varepsilon \left( \langle v_i h_j \rangle_{data} - \langle v_i h_j \rangle_{predict} \right) \quad (7)$$

$$\Delta a_i = \frac{\partial \log p(v)}{\partial a_i} = \varepsilon \left( \langle v_i \rangle_{data} - \langle v_i \rangle_{predict} \right) \quad (8)$$

$$\Delta b_j = \frac{\partial \log p(v)}{\partial b_j} = \varepsilon \left( \langle h_j \rangle_{data} - \langle h_j \rangle_{predict} \right) \quad (9)$$

where  $\varepsilon$  denotes the learning rate,  $\langle \square \rangle_{data}$  is the expectation of training after input data, and  $\langle \square \rangle_{predict}$  is the expectation of the model itself.

## 4. Improvement of the MRFP algorithm

### 4.1. Standard MRFP algorithm

Manta Ray Foraging Optimization (MRFO) [29] is a population-based meta-heuristic optimization algorithm that solves the optimization problem by modelling three foraging behaviours of manta rays. These three foraging behaviours are: chain foraging, spiral foraging and somersault foraging. Similar to other population-based algorithms, MRFO also generates individuals randomly in the search space to form an initial population. The mathematical models for each of the three foraging behaviours are presented next.

#### Chain foraging

Manta rays form a foraging chain by connecting their heads and tails in a line. While the first individual moves only towards the food, the rest of the individuals move not only towards the food, but also towards the individuals in the foraging chain located in front of them. The mathematical model of chain foraging is described as follows:

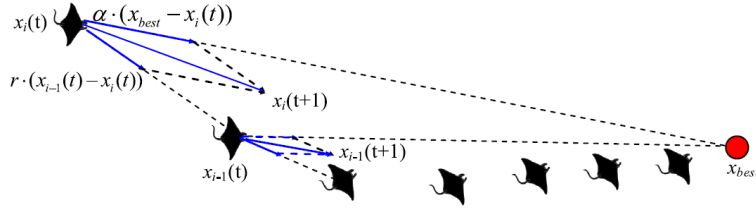


Figure 3. Chained foraging

$$X_i^{t+1} = \begin{cases} X_i^t + r_1 \cdot (X_{best}^t - X_i^t) + \alpha \cdot (X_{best}^t - X_i^t) & i = 1 \\ X_i^t + r_2 \cdot (X_{i-1}^t - X_i^t) + \alpha \cdot (X_{best}^t - X_i^t) & i = 2, 3, \dots, NP \end{cases} \quad (1)$$

$$\alpha = 2 \cdot r_3 \cdot \sqrt{|\log(r_4)|} \quad (2)$$

Where, denotes the position of the  $i$ th individual in generation  $t$ . The values of  $r_1, r_2, r_3, r_4$  are uniformly distributed random vectors.  $X_{best}^t$  denotes the plankton with the highest concentration, i.e., the optimal individual.  $NP$  is the population size, and  $\alpha$  is the weighting coefficient.

### Spiral foraging

When manta rays find plankton in deep water, they form long foraging chains and then move in a spiral towards the food. This behaviour is similar to the whale optimisation algorithm, but in addition to spiralling closer to the food, they also follow the individual in front of them. The mathematical model of spiral foraging can be given by the following equation:

$$X_i^{t+1} = \begin{cases} X_{best}^t + r_5 \cdot (X_{best}^t - X_i^t) + \beta \cdot (X_{best}^t - X_i^t) & i = 1 \\ X_{best}^t + r_6 \cdot (X_{i-1}^t - X_i^t) + \beta \cdot (X_{best}^t - X_i^t) & i = 2, 3, \dots, NP \end{cases} \quad (3)$$

$$\beta = 2e^{r_7 \frac{iter_{max} - iter + 1}{iter_{max}}} \cdot \sin(2\pi r_7) \quad (4)$$

where  $r_5, r_6$  are uniformly distributed random vectors with values ranging from 0 to 1.  $r_7$  is a uniformly distributed random number.  $\beta$  is a weight factor.  $iter_{max}$  and  $iter$  are the maximum number of iterations and the current number of iterations, respectively.

Food sources (optimal individuals) were mainly used as reference points for spiral foraging, which helped to fully

$$X_i^{t+1} = \begin{cases} X_{rand} + r_9 \cdot (X_{best}^t - X_i^t) + \beta \cdot (X_{best}^t - X_i^t) & i = 1 \\ X_{best}^t + r_{10} \cdot (X_{i-1}^t - X_i^t) + \beta \cdot (X_{best}^t - X_i^t) & i = 2, 3, \dots, NP \end{cases} \quad (6)$$

where  $X_{rand}$  is the randomly generated reference position in the search space.  $r_8, r_9$  and  $r_{10}$  are uniformly

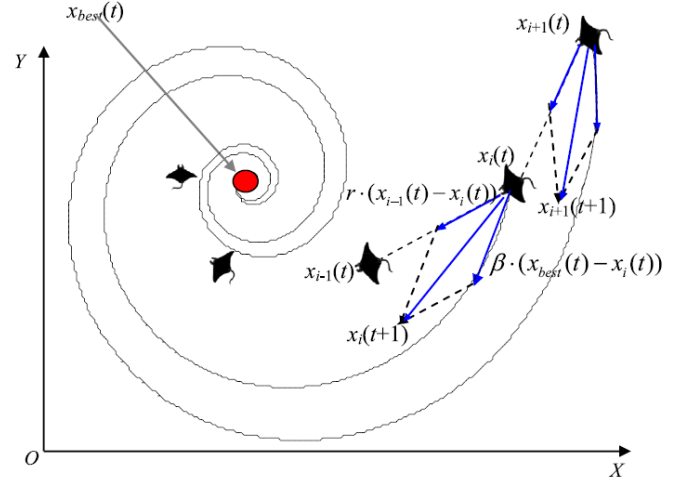


Figure 4. Spiral foraging

exploit the space around the optimal individuals. In addition, randomly generated locations in the search space were used as reference locations for spiral foraging in order to extend the search range. This allowed all individuals to search areas away from their current optimal position. The stochastic spiral foraging mechanism focuses primarily on exploration, allowing MRFOs to perform extensive global searches. The specific mathematical model is described below:

$$X_{rand} = lb + r_8 \cdot (ub - lb) \quad (5)$$

distributed random vectors with values ranging from 0 to 1.  $ub$  and  $lb$  are the upper and lower boundaries of the search space, respectively.

### Somersault foraging

In this stage, the food position is considered to be a fulcrum. Each individual flips around the pivot point, thus finding a new location. The mathematical model of this stage is represented as follows:

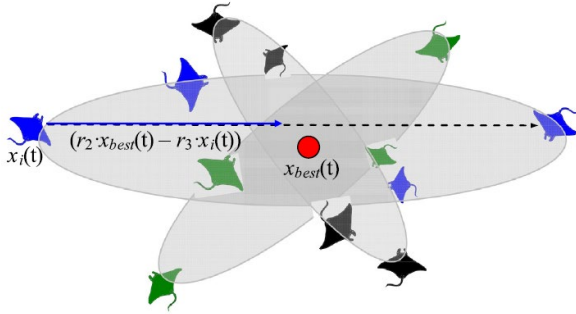


**Figure 5.** Somersault type foraging

$$X_i^{t+1} = X_i^t + S \cdot (r_{11} \cdot X_{best}^t - r_{12} \cdot X_i^t), i = 1, 2, \dots, NP \quad (7)$$

Among them,  $S$  is the coefficient affecting the rollover range of manta ray, which usually takes the value of 2.  $r_{11}$  and  $r_{12}$  are uniformly distributed random vectors, which take the value of 0~1.

The MRFO algorithm regulates the exploration and exploitation behaviour by controlling the variation of  $iter/iter_{max}$ . When  $iter/iter_{max} < rand$ , MRFO mainly performs the exploration behaviour, generating random food sources as reference points in the search space. When  $iter/iter_{max} \geq rand$ , the MRFO algorithm utilises the optimal individual as a reference point, which facilitates the exploitation of the algorithm. In addition, a random number is used to select either chain foraging or spiral foraging. After that, somersault foraging is performed.

### 4.2. Improvement strategies

In order to enhance the full-domain exploration capability of the MRFO algorithm and avoid the algorithm from falling into a local optimum, this paper adopts a good point set initialisation strategy [30], an adaptive control parameter strategy [31] and a distribution estimation strategy [32] to improve the manta ray foraging optimisation algorithm.

#### Good point set initialisation strategy

The quality of the initialised population of MRFO algorithm affects the solution optimisation speed of the algorithm, and an excellent population initialisation strategy can make the individuals of the population traverse the

whole search space more evenly, increase the population diversity and improve the convergence speed of the algorithm. In order to improve the population search diversity and make the population uniformly distributed in the search space, this paper proposes a good point set initialisation strategy to improve the initialisation method of MRFO algorithm. Suppose  $G_s$  is a unit cube in  $s$ -dimensional Euclidean space, if  $r \in G_s$ , for:

$$P_n(k) = \left[ \left( r_1^{(n)} \cdot k \right), \left( r_2^{(n)} \cdot k \right), \dots, \left( r_s^{(n)} \cdot k \right) \right], 1 \leq k \leq n \quad (8)$$

Its deviation is satisfied:

$$\phi(n) = C(r, \varepsilon) n^{\varepsilon-1} \quad (9)$$

Then  $P_n(k)$  is called the set of good points and  $r$  is the good point.  $\left( r_1^{(n)} \cdot k \right)$  represents the fractional part,  $\varepsilon$  is any positive number,  $C(r, \varepsilon)$  is a constant related only to  $r, \varepsilon$ ,  $n$  denotes the number of points, and  $r$  is:

$$r = \{ 2 \cos(2\pi k/p), 1 \leq k \leq s \} \quad (10)$$

where  $p$  is the smallest prime number satisfying  $(p-3)/2 \geq s$ . The initialised population distribution graph using the set of good points is shown in Figure 3.

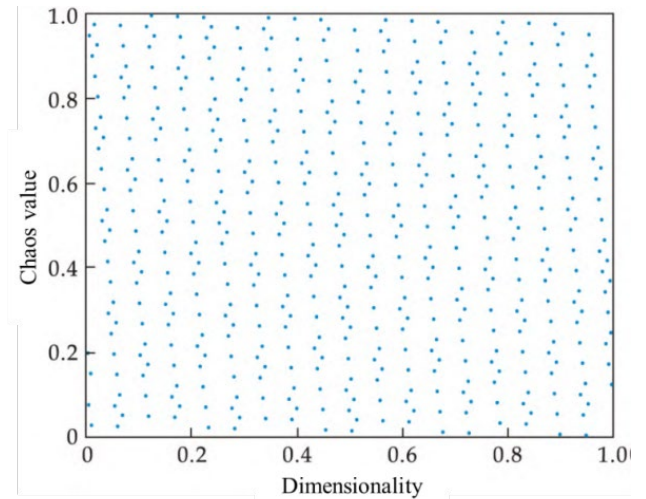


**Figure 6.** Distribution of initialised populations in the good point set

#### Adaptive control parameter strategy

The MRFO algorithm regulates exploration and exploitation behaviour by controlling changes in  $iter/iter_{max}$ .  $iter/iter_{max}$  The change of is a linearly

increasing variable that does not accurately reflect and adapt to the complex nonlinear search process. Nonlinear parameter control strategy style is an effective measure to prevent the algorithm from maturing prematurely. In this paper, an adaptive control parameter strategy with a mixture of sine and cosine functions is proposed, as shown in Figure 7, and the specific mathematical model is as follows:

$$Coef = \sin\left(\frac{\pi \cdot iter}{2iter_{max}}\right)^{\left(2.5\cos(iter/iter_{max})^3\right)} \quad (11)$$

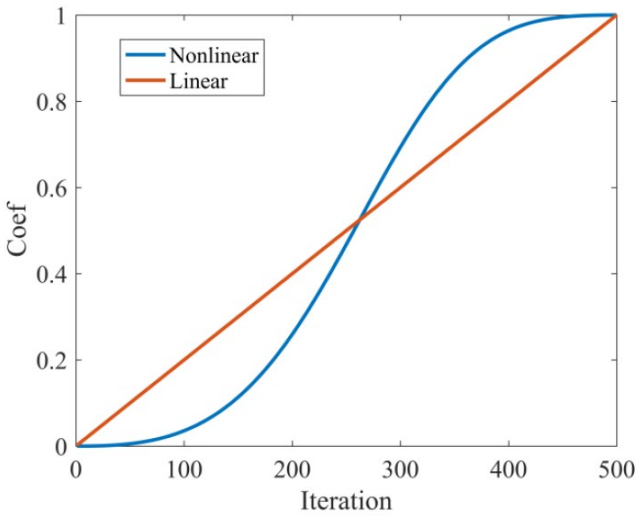


**Figure 7.** Different control parameters

As can be seen from Figure 7, the new strategy focuses more on global search in the early stages to avoid the algorithm from falling into a local optimum. In the later stages, the algorithm performs more local exploitation behaviour, which helps the algorithm to accelerate convergence. When MRFO performs somersault foraging, the parameter  $S$  is constant, which is not conducive to the effective execution of the algorithm. In the early stages of optimisation, the algorithm performs more exploratory behaviour, so the parameter  $S$  needs to become large enough to search more space. In the later stages of iteration, the algorithm needs to be more precise in its exploitation, and smaller values of the parameter  $S$  are required. Therefore, this paper proposes a linearly decreasing strategy for the parameter  $S$  with the following mathematical model:

$$S = (S_{min} - S_{max}) \cdot iter / iter_{max} + S_{max} \quad (12)$$

Where  $S_{min}$  and  $S_{max}$  are the minimum and maximum values of the parameter  $S$ .

### Distribution estimation strategy

The chained foraging strategy of the standard MRFO algorithm uses the optimal individual and neighbouring individuals for position updating, which can easily lead to premature convergence of the algorithm. If the optimal individual has already fallen into the local optimum, the chaining rule will cause all subsequent individuals to approach the local optimal individual. In order to improve the performance of the algorithm, this paper proposes a distribution estimation strategy with the following mathematical model:

$$X_i^{t+1} = mean + y \quad y \square N(0, Cov) \quad (13)$$

$$mean = (X_{esp} + X_{mean}^t + X_i^t) / 3 \quad (14)$$

$$Cov(i) = \frac{1}{NP/2} \sum_{i=0}^{NP/2} (X_i^{t+1} - X_{mean}^t) \times (X_i^t - X_{mean}^t)^T \quad (15)$$

$$X_{mean}^t = \sum_{i=1}^{NP/2} \omega_i \times X_i^t \quad (16)$$

$$\omega_i = \frac{\ln(NP/2 + 0.5) - \ln(i)}{\sum_{i=1}^{NP/2} \ln(NP/2 + 0.5) - \ln(i)} \quad (17)$$

where  $X_{mean}^t$  denotes the weighted position of the dominant population,  $\omega$  denotes the weighting coefficients in the dominant population in descending order of fitness values, and  $Cov$  denotes the weighted covariance matrix of the dominant population. The distribution estimation strategy with chained foraging measurement class was randomly selected for execution.

### 4.3. Improvement of MRFP algorithm step by step process

Based on the improvement strategy and optimisation process, the GoodADMRFO algorithm (MRFO based on Good point set, Adaptive control parameter strategy and Distribution estimation strategy) pseudo-code is shown in Figure 8 with the following steps. :

Algorithm 1 GoodADMRFO algorithm	
1	Set parameters of GoodADMRFO algorithm;
2	Initialize population of GoodADMRFO algorithm based on good point set strategy;
3	Calculate fitness value;
4	For t = 1:iter_max
5	Calculate mean and Cov of distribution estimation strategy;
6	if rand<0.5
7	if Coef>0.5
8	Carry out Cyclone foraging strategy based on best point;
9	else
10	Carry out Cyclone foraging strategy based on random point;
11	end
12	else
13	if 0.5>rand
14	Carry out Chain foraging strategy;
15	else
16	Carry out Distribution estimation strategy;
17	end
18	Control position boundary, and calculate fitness;
19	Carry out Somersault foraging strategy;
20	Control position boundary, and calculate fitness;
21	end
22	Output best individual and its fitness.

**Figure 8.** Pseudo-code of GoodADMRFO algorithm

Step 1: Initialise the population position using the good point set strategy, set the maximum number of iterations and other parameters;

Step 2: Calculate the fitness value and record the current optimal individual;

Step 3: Update the mean and Cov of the distribution estimation strategy;

Step 4: Population position update based on spiral foraging with improved chain foraging strategy. If rand<0.5 and Coef>0.5, spiral foraging strategy based on optimal individuals is used; if rand<0.5 and Coef≤0.5, spiral foraging strategy based on random individuals is used; and if rand≥0.5, chained foraging strategy based on distribution estimation strategy is used;

Step 5: Control the position boundary, calculate the fitness value and update the optimal individual;

Step 6: Location update based on somersault foraging strategy;

Step 7: Control the position boundary, calculate the fitness value and update the optimal individual;

Step 8: Determine whether the number of iterations reaches the maximum number of iterations. If the maximum number of iterations is reached, carry out the output of the optimal solution and optimal value; otherwise, go to step 3.

## 5. Ideas for tumour diagnosis methods based on the GoodADMRFO algorithm for optimising deep confidence networks

Combining GoodADMRFO and deep confidence network, this section proposes a tumour diagnosis method based on GoodADMRFO algorithm to improve DBN network.

### 5.1. Decision variables and objective functions

The traditional iterative approach to DBN network optimisation can easily cause the optimisation of DBN network parameters to fall into local optimum. In order to overcome the above problems, this paper adopts the GoodADMRFO algorithm to optimise the DBN network parameters. The optimisation decision variable of the GoodADMRFO algorithm is  $\theta = (\omega, a, b)$ .

In order to overcome the DBN training accuracy, the Error, F-score, and FPR functions are used as the objective

functions of the GoodADMRFO-DBN algorithm and are calculated as follows:

$$\min Fitness(X) = \alpha \cdot Error + \beta \cdot \frac{1}{F-score} + \gamma \cdot FPR \quad (18)$$

$$Error = 1 - Accuracy \quad (19)$$

$$Accuracy = \frac{TP + TN}{TP + TN + FP + FN} \quad (20)$$

$$FPR = \frac{FP}{TN + FP} \quad (21)$$

$$Precision = \frac{TP}{TP + FP} \quad (22)$$

Among them,  $\alpha + \beta + \gamma = 1$  ;  $\alpha = 0.4$  ,  $\beta = 0.4$  ,  $\gamma = 0.2$  .

### 5.2. Steps and processes

The tumour diagnosis model based on GoodADMRFO algorithm optimized DBN network is mainly based on the mapping relationship between features and recognition types with tumour diagnostic features as input and diagnostic recognition types as output. The flowchart of the tumour diagnosis method based on GoodADMRFO-DBN algorithm is shown in Figure 9. The specific steps are as follows:

Step 1: According to the state of the tumour, the tumour diagnostic features are extracted; the features are dimensionality reduced using principal component analysis; the dataset is divided into a training set, a validation set and a test set;

Step 2: The GoodADMRFO algorithm is used to encode the initial DBN parameters, and also initialise the algorithm parameters such as the population parameters and the number of iterations; the population is initialised and the objective function value is calculated;

Step 3: Update the mean and Cov of the distribution estimation strategy; if  $rand < 0.5$  and  $Coef > 0.5$ , use the spiral foraging strategy based on the optimal individual; if  $rand < 0.5$  and  $Coef \leq 0.5$ , use the spiral foraging strategy based on the random individual; if  $rand \geq 0.5$ , use the chain foraging strategy based on the distribution estimation strategy of chain foraging strategy; calculate the fitness value and update the optimal solution;

Step 4: Based on the somersault foraging strategy, the position is updated; the fitness value is calculated and the optimal solution is updated;

Step 5: Determine whether the termination condition is satisfied, if so, exit the iteration, output the optimal DBN network parameters, and execute step 3, otherwise continue to execute step 6;

Step 6: Decode the GoodADMRFO-based optimised DBN parameters, obtain the optimal DBN parameters, and construct the GoodADMRFO-DBN-based tumour diagnosis model;

Step 7: Diagnose and identify the current test set using the trained tumour diagnostic model, and output the corresponding diagnostic results.

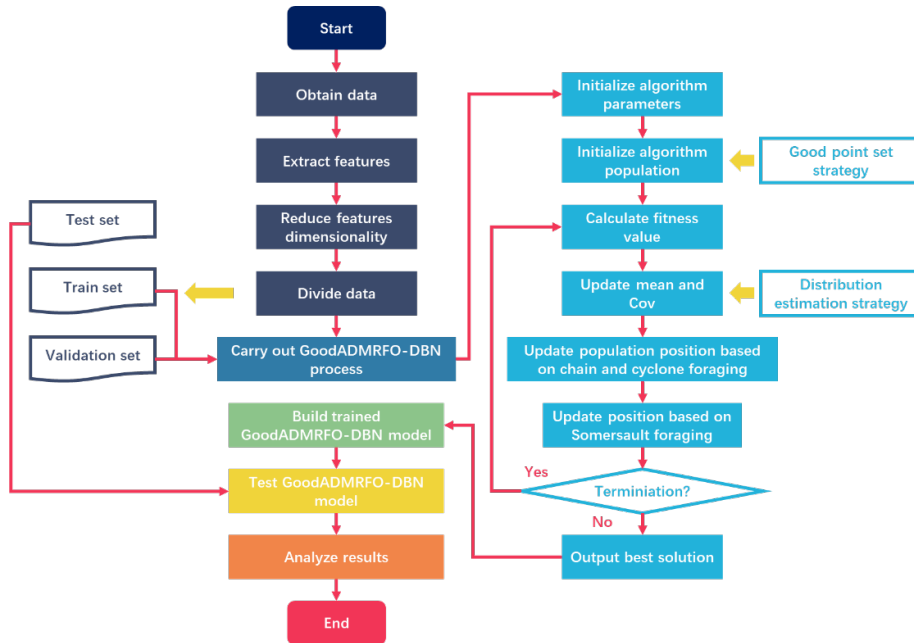


Figure 9. Flowchart of GoodADMRFO-DBN based tumour diagnosis approach

## 6. Experiments and analysis of results

In order to verify the accuracy and timeliness of the tumour diagnostic model proposed in this paper, five diagnostic algorithms were selected for comparison, and the specific parameter settings of each algorithm are shown in

Table 1. The data were mainly obtained from the sample data of breast tumour diagnostic cases in the UCI Machine Learning Library. The experimental simulation environment is Windows 10, CPU is 2.80GHz, 8GB memory, programming language Matlab2017b.

Table 1. Parameter settings of English teaching quality evaluation methods

arithmetic	parameterisation
DBN	Three hidden layers with 100, 100, 100 nodes in each layer
MRFO-DBN	Three hidden layers, with the number of nodes being determined by Section 6.1 and the number of populations being determined by Section 6.1
MRFO-1-DBN	Three hidden layers, the number of nodes is determined by Section 6.1, the number of populations is determined by Section 6.1, and MRFO does not use a good point set initialisation strategy
MRFO-2-DBN	Three hidden layers, the number of nodes is determined by section 6.1, the number of populations is determined by section 6.1, and MRFO does not use an adaptive control parameter strategy
MRFO-3-DBN	Three hidden layers, the number of nodes is determined by Section 6.1, the number of populations is determined by Section 6.1, and the MRFO does not use a distribution estimation strategy
GoodADMRF-DBN	Three hidden layers, the number of nodes is determined by Section 6.1, the number of populations is determined by Section 6.1, and MRFO does not use a good point set initialisation strategy

### 6.1. Parameter setting analysis

In order to analyse the impact of the population size of MRFO algorithm and the number of hidden layer nodes of DBN network on the tumour diagnosis method, this paper compares and analyses the performance of the tumour diagnosis method under the conditions of different population sizes and different numbers of hidden layer nodes of the network, respectively. Figure 10 gives a graph of the impact of different population sizes and different numbers of network hidden layer nodes on diagnosis accuracy, and Figure 11 gives a graph of the impact of different population sizes and different numbers of network hidden layer nodes on diagnosis time.

As can be seen from Figure 10, as the number of populations of the optimization algorithm increases, the accuracy of tumour diagnosis also gradually increases; as the number of DBN hidden layer nodes increases, the accuracy of tumour diagnosis also gradually increases; when the number of populations increases to 70, the increase in the accuracy of tumour diagnosis becomes slow, and even the performance decreases; when the number of hidden nodes of the DBN network increases to 80, the effect of the increase in the accuracy of tumour diagnosis is not obvious. As can be seen from Figure 11, with the increase in the number of populations of the optimization

algorithm, the tumour diagnosis time also increases gradually; with the increase in the number of hidden nodes of DBN, the tumour diagnosis time also increases gradually; when the number of populations is increased to 90, the tumour diagnosis time change no longer increases and tends to be stable; when the number of hidden nodes of DBN network is increased to 80, the tumour diagnosis time increases more quickly. In summary, the intelligent optimisation algorithm selected in this paper has a population size of 80 and the number of hidden nodes of DBN network is 90.

Figure 10 gives the results of tumour cancer diagnosis based on each algorithm. As can be seen from Figure 10, comparing the GoodADMRF-DBN and DBN algorithms shows that the optimisation and improvement strategy improves the diagnostic accuracy of the DBN and MRFO-DBN algorithms; comparing the MRFO-DBN and MRFO-1-DBN algorithms shows that the good point set initialisation strategy improves the diagnostic accuracy of the MRFO-DBN; comparing MRFO-DBN and MRFO-2-DBN shows that the adaptive control parameter strategy improves the MRFO-DBN diagnostic accuracy; comparing MRFO-DBN with MRFO-3-DBN shows that the distribution estimation strategy improves the MRFO-DBN diagnostic accuracy. Meanwhile, GoodAD-based MRFO-DBN has the highest diagnostic identification accuracy.

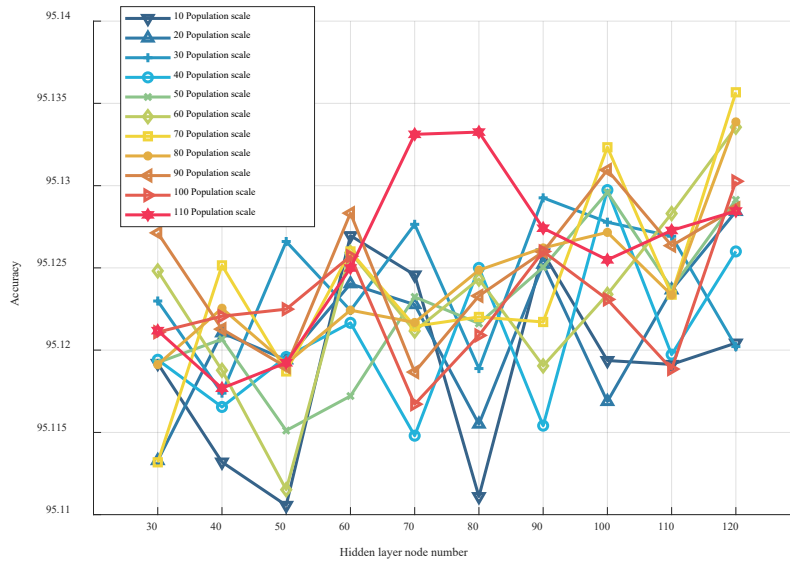


Figure 10. Effect of different population sizes and number of hidden nodes on diagnostic accuracy

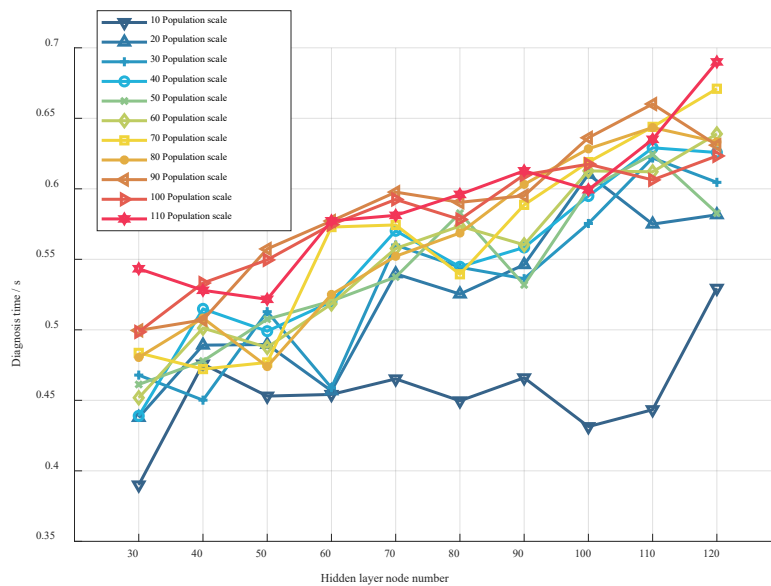
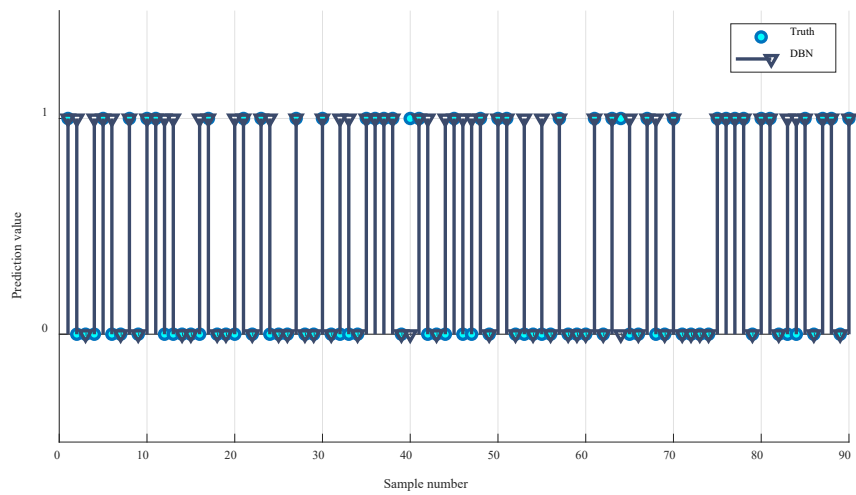


Figure 11 Effect of different population sizes and number of hidden nodes on diagnosis time

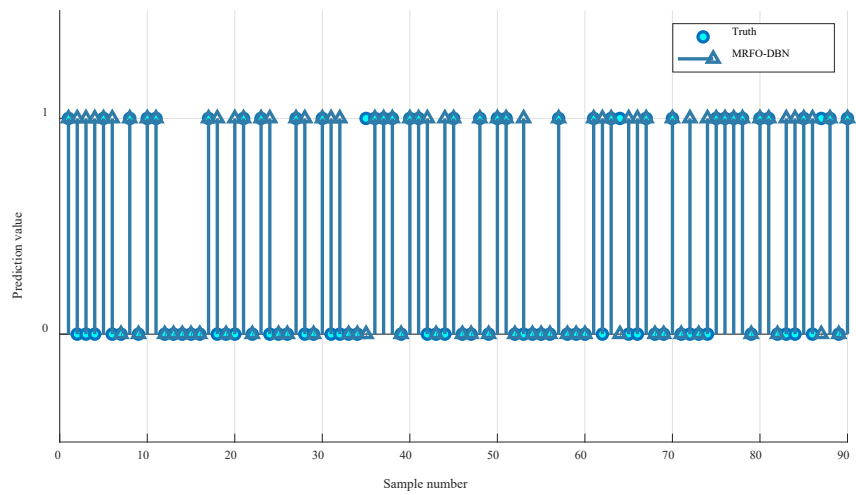
## 6.2. Experimental prediction performance analysis

In order to verify the effectiveness and superiority of the tumour cancer diagnosis method based on the GoodADMRF0-DBN algorithm, GoodADMRF0-DBN is compared with five other models such as DBN, MRFO-

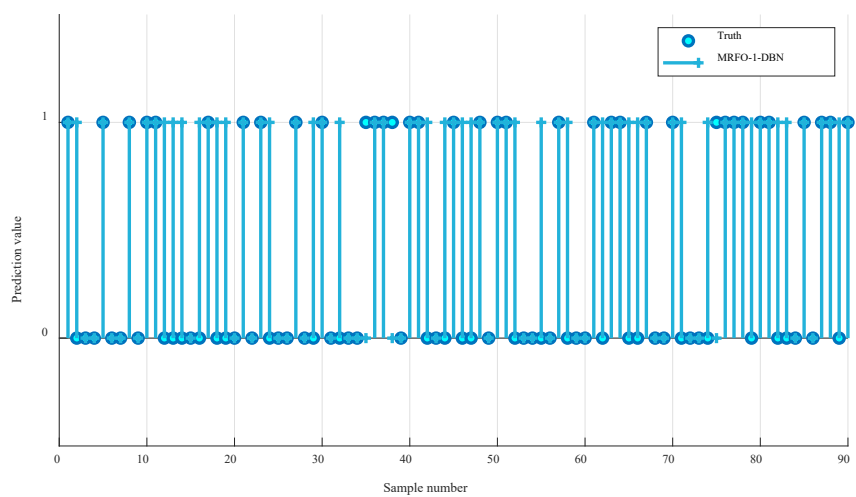
DBN, MRFO-1-DBN, MRFO-2-DBN, MRFO-3-DBN, and the performance results of each model are shown in Figure 12, Figure 13 and Figure 14.



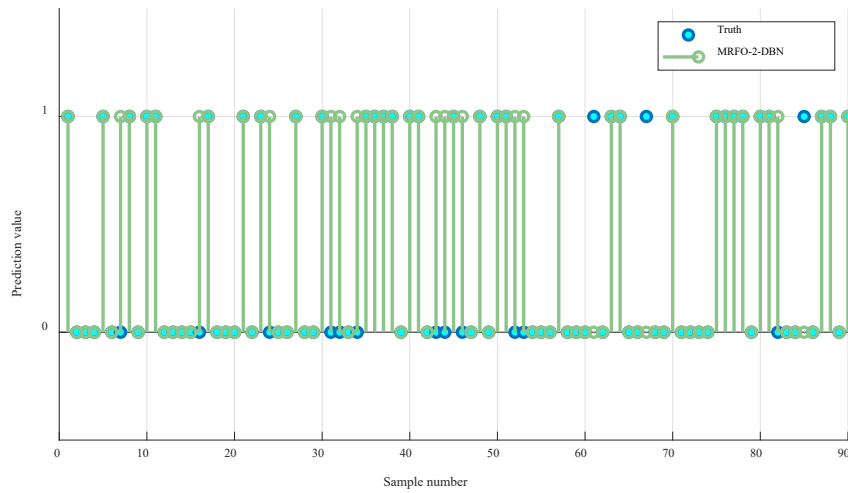
(a) DBN



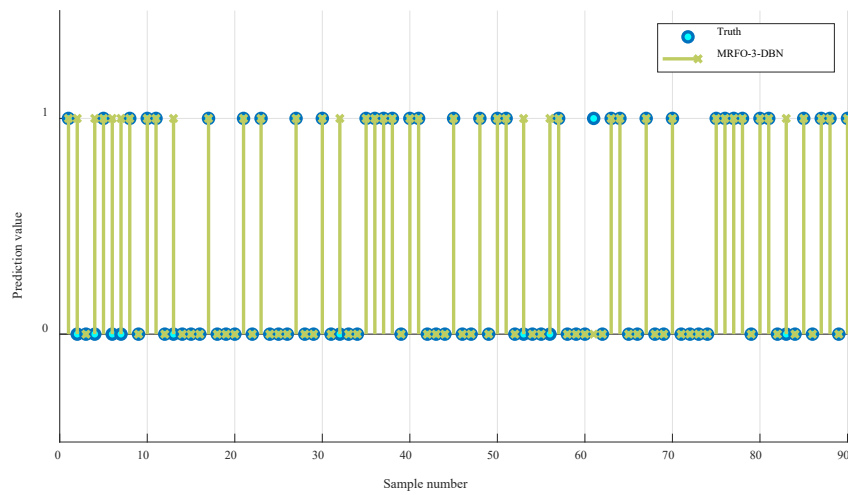
(b) MRFO-DBN



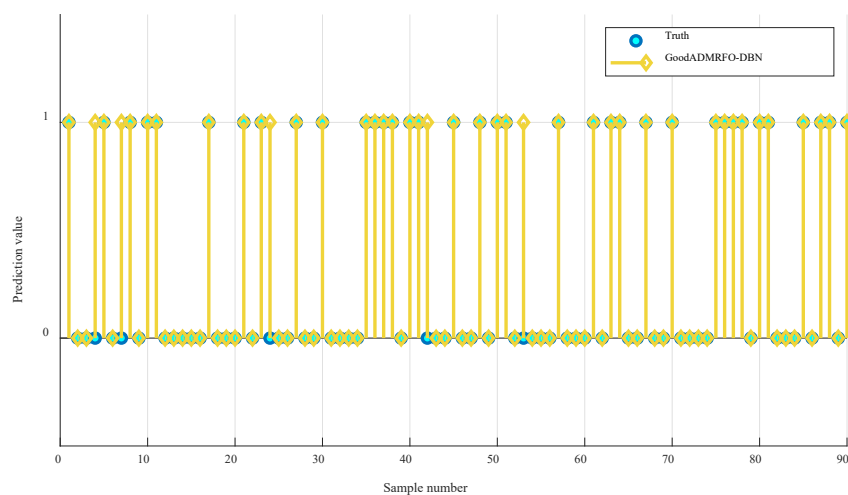
(c) MRFO-1-DBN



(d) MRFO-2-DBN



(e) MRFO-3-DBN



(f) GoodADMRFO-DBN

**Figure 12.** Tumour cancer diagnosis results based on each algorithm

In order to further verify the superiority of the tumour diagnosis method based on the GoodADMRFO-DBN

algorithm, the results of the diagnostic performance of each algorithm are statistically given in this section, as shown in

Figure 13 and Figure 14. From Figure 13, it can be seen that the diagnostic accuracy mean value of GoodADMRFO-DBN algorithm based on GoodADMRFO-DBN algorithm is larger than other algorithms, and the accuracy standard deviation is smaller than other algorithms, and the diagnostic effect is better than other algorithms; the diagnostic time mean value of GoodADMRFO-DBN algorithm based on GoodADMRFO-DBN algorithm is smaller than DBN and MRFO algorithms, but larger than

MRFO-1-DBN and MRFO-2-DBN, MRFO-3-DBN algorithms, and the standard deviation of time is better than the other algorithms, which shows that the stacking of the three strategies may increase the computational burden, but the robustness becomes better. In conclusion, the tumour diagnosis method based on GoodADMRFO-DBN algorithm works better than other algorithms and meets the real-time requirements.

Algorithm	Accuracy mean	Accuracy SD	Time mean	Time SD
DBN	89.10%	1.77	0.0244	0.0019
MRFO-DBN	92.32%	1.99	0.0092	0.0017
MRFO-1-DBN	93.32%	1.23	0.0041	0.0008
MRFO-2-DBN	93.76%	1.19	0.0033	0.0016
MRFO-3-DBN	94.11%	0.67	0.0032	0.0002
GoodADMRFO-DBN	95.57%	0.38	0.0052	0.0001

**Figure 13.** Comparison of tumour diagnosis accuracy and time analysis based on each algorithm

As can be seen from Figure 14, the diagnostic optimisation process based on the GoodADMRFO-DBN algorithm is better than MRFO-DBN, MRFO-1-DBN, MRFO-2-DBN, MRFO-3-DBN, with a faster convergence

speed and better convergence accuracy than the other algorithms. In conclusion, the optimisation of tumour diagnosis based on GoodADMRFO-DBN algorithm has faster convergence speed and better convergence accuracy.

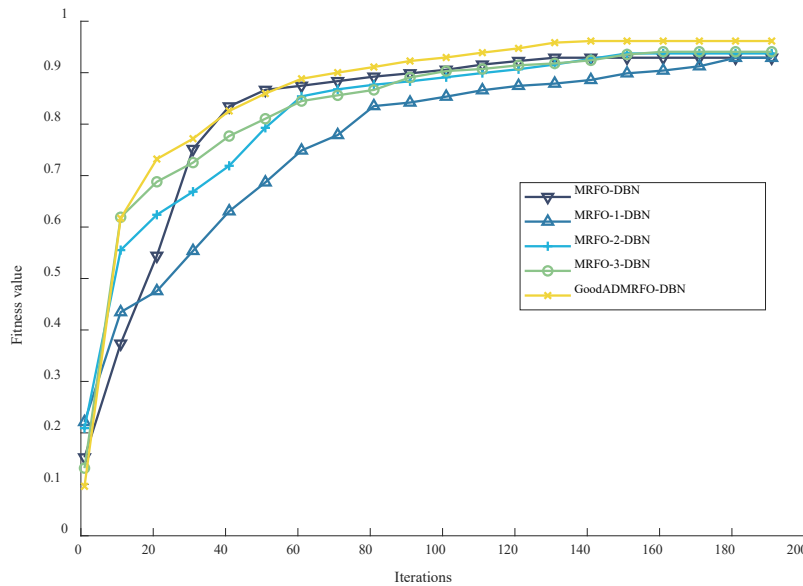


**Figure 14.** Convergence curve analysis of tumour diagnosis accuracy based on each optimisation algorithm

## 7. Conclusion

Aiming at the defects of incomplete features, low accuracy and low real-time performance of tumour diagnosis methods, this paper proposes a tumour diagnosis method based on the improved MRFO algorithm to improve the optimization process of DBN network parameters. The method extracts diagnostic data features by analysing the tumour diagnosis identification problem. The manta ray foraging optimisation algorithm is improved by combining the good point set initialisation strategy, adaptive control parameter strategy and distribution estimation strategy, and the parameters of the depth confidence network are optimised using the improved manta ray foraging optimisation algorithm to construct a tumour diagnosis model. Simulation experiments are carried out using breast tumour diagnostic feature data, and the following conclusions are drawn:

(1) By comparing the diagnostic performance of the MRFO-DBN and DBN algorithms, the MRFO algorithm can improve the diagnostic accuracy of DBN;

(2) By comparing the diagnostic performance of GoodADMRF-DBN with MRFO-DBN, MRFO-1-DBN, MRFO-2-DBN, and MRFO-3-DBN algorithms, and optimising the improvement strategies to further improve the diagnostic model accuracy;

(3) GoodADMRF-DBN diagnostic time meets real-time requirements.

The time performance of the diagnostic model proposed in this paper is not good, and further improvement of GoodADMRF-DBN diagnostic time is the next research focus.

## References

- [1] Kirchweger P , Wundsam H V , Rumpold H .Circulating tumour DNA for diagnosis, prognosis and treatment of gastrointestinal malignancies[J].World journal of clinical oncology, 2022(6).
- [2] Deng, Dajun. World Cancer Report 2020 - Adapting Cancer Prevention Responses to New Trends in Cancer Epidemics. Electronic Journal of Comprehensive Cancer Therapy[J]. 2002(03), 27-32.
- [3] Park W , Maeng S W , Mok J W , Choi M , Cha H J , Joo C K. Hydrogel Microneedles Extracting Exosomes for Early Detection of Colorectal Cancer[J]. Biomacromolecules, 2023.
- [4] Dolganova I N , Varvina D A , Shikunova I A , Alekseeva A I , Karalkin P A , Kuznetsov M R. Proof of concept for the sapphire scalpel combining tissue dissection and optical diagnosis[J].Lasers in surgery and medicine. 2022(4):54.
- [5] Aiwen S .Clinical role of serum tumour markers SCC, NSE, CA 125, CA 19-9, and CYFRA 21-1 in patients with lung cancer[J]. .
- [6] Li J , Yan Y , Wang G , Huang Z. Hypoxia-inducible factor-2 $\alpha$ and its missense mutations:potential role in HCC diagnosis,progression,and prognosis and underlying mechanism[J]. Oncology and Translational Medicine:English Edition, 2022, 8(6):267-275.
- [7] Pinto G V , Senthilkumar K , Rai P , Kabekkodu S P , Karunasagar I, Kumar B K. Current methods for the diagnosis of leptospirosis: Issues and challenges[J] . Journal of Microbiological Methods, 2022, 195:106438.
- [8] Nian-Lun Z , Qin K , Li-Ying B , Bing-Xue J. The value of combined detection of serum tumor markers in the diagnosis and prognosis of non-small cell lung cancer[J].Chinese Journal of Convalescent Medicine, 2023, 32(7):763-768.
- [9] Krzysztof Szymoński, Chmura U , Lipiec E , Adamek D. Vibrational spectroscopy-are we close to finding a solution for early pancreatic cancer diagnosis?[J]. World Journal of Gastroenterology:English Edition, 2023, 29(1):96-109.
- [10] Tyler C , Neil M N , Alexis J , Sarah R, Erin W. The effects of educational interventions and the COVID-19 pandemic on the time to diagnosis in pediatric patients with primary central nervous system tumours[J].Neuro-Oncology Practice, 2023(5):5.
- [11] Zhang Y C , Li M , Jin Y M , Xu J X, Huang C C. Radiomics for differentiating tumor deposits from lymph node metastasis in rectal cancer[J]. World Journal of Gastroenterology: English Edition, 2022(029):028.
- [12] Minoshima A , Sugita S , Segawa K , Aoyama T, Ito M, Daimon F. Usefulness of cell block examination for the cytological diagnosis of thoracic SMARCA4- deficient undifferentiated tumour: a case report[J].Diagnostic cytopathology, 2023.
- [13] Rakotoarivo T , Tomboravo C , Razakanaivo M , Raharisolo C, Rafaramino F. Advanced Cutaneous Scalp Eccrine Adenocarcinoma, Diagnosis and Treatment Challenges: a Case Report[J]. Cancer Therapy (English), 2023, 14(1):1-5.
- [14] Rodanthi Sfakiotaki M , Sergia Liasi B , Eleni Papaiakevou B , Vraka I, Vakaki M, Koumanidou C. Juvenile Granulosa Cell Tumor of the Testis: A Preoperative Approach of the Diagnosis with Ultrasound[J]. 2023, 7(4):409-411.
- [15] Farzahna M , Raal F J .Unravelling the Whipple Triad: Non-Islet Cell Tumor-Induced Hypoglycemia[J].JCEM Case Reports. 2024(2):2.
- [16] Yan Y W , Liu X K , Zhang S X , Tian Q F. Real-world 10-year retrospective study of the guidelines for diagnosis and treatment of primary liver cancer in China[J]. World Journal of Gastrointestinal Oncology:English Edition(Electronic), 2023, 15(5):859-877.
- [17] Juan L. The Comparative Study on Common Breast Imaging Diagnosis Methods[J]. Foreign language edition: medicine and health, 2022(1):169-172.
- [18] Inoue F , Hirata D , Iwatate M , Hattori S, Fujita M, Sano W. New application of endocytoscope for histopathological diagnosis of colorectal lesions [J ]. World Journal of Gastrointestinal Endoscopy: English Edition (electronic version), 2022(008):014.
- [19] Rossi R E , Elvevi A , Gallo C , Palermo A, Invernizzi P, Massironi S. Endoscopic techniques for diagnosis and treatment of gastroentero-pancreatic neuroendocrine neoplasms:Where we are[J]. World Journal of Gastroenterology: English Edition, 2022(026):028.
- [20] Asiri A A , Iqbal A , Ferzund J , Ali T, Aamir M, Alshamrani K A. A Novel Hybrid Machine Learning Approach for Classification of Brain Tumor Images[J]. Computers, Materials and Continuum (English), 2022.
- [21] Huang Z , Huang Z , Zhao Y , Zhao Y, Liu Y, Liu Y. AMF-Net: An adaptive multisequence fusing neural network for multi-modality brain tumor diagnosis[J]. Biomedical Signal Processing and Control, 2022, 72:103359-.
- [22] Bibikova M , Fan J .Liquid biopsy for early detection of lung

- cancer[J]. *Respiratory and Critical Care Medicine (English)*, 2023, 01(04):200-206.
- [23] Yin Z , Zhang J .Cross-subject recognition of operator functional states via EEG and switching deep belief networks with adaptive weights[J]. *Neurocomputing*, 2017, 260(oct.18):349-366.
- [24] Wang Qianhe,Li Renwang. Optimisation of low carbon turning parameters based on improved whale optimisation algorithm[J]. *Modelling and Simulation*, 2023, 12(6):10.
- [25] Wang X , Zhang W .The Janus of Protein Corona on nanoparticles for tumour targeting, immunotherapy and diagnosis[J].*Journal of Controlled Release*,. 2022, 345:832-850.
- [26] Aiwen S .Clinical role of serum tumor markers SCC, NSE, CA 125, CA 19-9, and CYFRA 21-1 in patients with lung cancer[J].*Laboratory Medicine*, 2023(6). 6.
- [27] Katherine L , Fei D .The success rates of clinical cancer next-generation sequencing based on pathologic diagnosis: experience from a single academic laboratory[J].*American Journal of Clinical Pathology*, 2023(5):5.
- [28] Lin W C , Tsai C F , Zhong J R .Deep learning for missing value imputation of continuous data and the effect of data discretisation[J].*Knowledge-Based Systems*, 2022, 239:108079-.
- [29] Weiguo Z, Zhengxin Z, Liying W. Manta ray foraging optimization: an effective bio-inspired optimizer for engineering applications[J]. *Engineering Applications of Artificial Intelligence*, 2020, 87: 103300.
- [30] Du J , Gao Y .Domain adaptation and Summary Distillation for Unsupervised Query Focused Summarization[J].*IEEE Transactions on Knowledge and Data Engineering*, 2023.
- [31] Guo Jianyi,Fan Youping. Adaptive control strategy for VSG parameters based on improved particle swarm algorithm[J]. *Journal of Electrical Machines and Control*, 2022, 26(6):11.
- [32] Usman H M , Elshatshat R , El-Hag A H .Distribution Transformer Remaining Useful Life Estimation Considering Electric Vehicle Penetration[J].*IEEE Transactions on Power Delivery*, 2023.